Hydroxyapatite coating modifies implant membrane formation,

Controlled micromotion studied in dogs

Kjeld Søballe[1,2], Helle Brockstedt-Rasmussen[3], Ebbe Stender Hansen[1,2] and Cody Bünger[1]

We studied the influence of controlled micromovements between bone and porous titanium alloy implants with and without hydroxyapatite coating. A dynamically loaded unstable device producing approximately 150-μm axial translation of knee implants during each gait cycle was developed. Stable implants served as controls. Matched stable and unstable implants with either porous titanium (Ti) or hydroxyapatite (HA) coating surrounded by a gap of 0.75 mm were inserted into the weight-bearing regions of the medial femoral condyles in 14 mature dogs. Histologic analysis after 4 weeks showed a fibrous membrane surrounding both types of implants subjected to micromovements, whereas various amounts of bone ingrowth was obtained in the stable implants. The membrane around unstable HA implants was thinner than that around unstable Ti implants. Islands of fibrocartilaginous tissue characterized the membrane around unstable HA implants, whereas fibrous connective tissue surrounded unstable Ti implants. The collagen concentration of the fibrous membranes was higher around unstable HA implants compared with Ti implants. Instability reduced the shear strength of the implants. However, the shear strength of unstable HA implants exceeded that of the Ti implants, both unstable and stable. The greatest shear strength was obtained by stable HA implants, i.e., tenfold greater than that of stable Ti implants. The gap-healing capacity around stable HA implants increased toward the HA surface, and was greater than that around Ti implants.

Our study demonstrates that micromovements between bone and implant inhibit bone ingrowth and lead to the development of a fibrous membrane. The superior fixation of unstable HA implants compared with unstable Ti implants may be ascribed to the presence of fibrocartilage, a higher collagen concentration, and radiating orientation of collagen fibers in the membrane. The strongest mechanical anchorage and the greatest amount of bone ingrowth was obtained by stable implants coated with hydroxyapatite.

University of Århus, [1]Biomechanics Laboratory at Orthopedic Hospital, [2]Institute of Experimental Clinical Research, and [3]Institute of Pathology, Århus Amtssygehus, Denmark
Correspondence: Dr. Kjeld Søballe, M.D., Biomechanics Laboratory, Orthopedic Hospital, Randersvej 1, DK-8200 Århus N, Denmark. Tel +45 86 11 24 00 (private), +45 86 12 55 55 (hospital)
Submitted 91-03-05. Accepted 91-08-17

Cadaver studies of knee and hip prostheses have demonstrated micromovements between bone and implant in the range of 100–600 μm at loads in the low physiologic range (Shimagaki et al. 1988, Strickland et al. 1988, Volz et al. 1988, Branson et al. 1989, Vanderby et al. 1989, Burke et al. 1991). We have recently reported a dog model for studies of controlled movements between bone and implant (Søballe et al. 1990, 1992) where a fibrous membrane occurred around implants subjected to micromovements of 500 μm, whereas bone ingrowth was found around stable control implants. The aim of the present study was to investigate whether or not movements of 150 μm between bone and implant were sufficient to affect bone ingrowth into Ti- and HA-coated porous implants using the new model with controlled implant movements during each gait cycle.

Material and methods

Experimental design

We used 14 mature Labrador retrievers, which were 2 (1–4) years of age and weighed 28 (21–35) kg. Preoperative radiographic screening of both knees ensured that all the animals were skeletally mature and lacked osseous abnormalities. Implantation of stable and unstable implants with Ti-porous coating was performed in the weight-bearing region of the medial femoral condyles in 7 dogs. In a sex-, age-, and weight-matched group of another 7 dogs, HA-coated implants were inserted. Stable and unstable implants were alternated randomly between the right and the left knee. The dogs were killed after 4 weeks, and the results were evaluated by means of push-out tests,

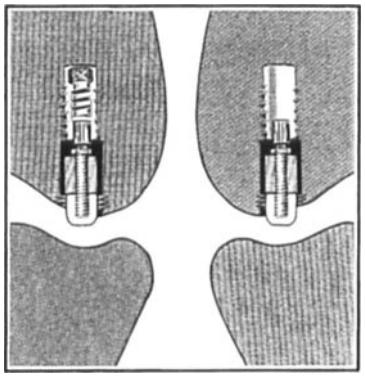

Figure 1. The principle for producing micromovements. The dynamic device consists of an implantable hollow screw with a spring and a piston on which the test implant is mounted. A polyethylene plug projects above the femoral articular cartilage. A titanium ring is mounted subchondrally and serves as a bearing and centralizer for the polyethylene plug. All the metal components are manufactured from titanium alloy (Ti-6Al-4V). The system is inserted into the weight-bearing part of the femoral condyle. When the knee is loaded during gait, load transfer from the tibial part of the knee will displace the implant in the axial direction and tighten the spring. When the leg is unloaded, the tightened spring will move the implant back to the initial position. Thus, a controlled movement will occur during each gait cycle. In the contralateral knee, a stable device is used as a control.

histomorphometric analysis, polarizing microscopy, scanning electron microscopy, UV fluorescence microscopy, collagen analysis, and transmission electron microscopy with microanalysis.

Dynamic device

The principle of producing micromovements is shown in Figure 1. A more detailed description has been given previously (Søballe et al. 1990, 1992). In the present study, movement was preset to approach 150 µm. Mechanical testing of the device was performed before and after implantation using a universal Instron testing machine (Søballe et al. 1992). The stiffness of the springs was adjusted until the desired elasticity (approximately 14 N/mm) and a preload (approximately 2.5 N) were obtained. After 4 weeks, the loaded devices were removed from the bone and tested mechanically using an identical procedure (Table 1). Preload, stiffness, and displacement of devices with HA and Ti implants were equal. In addition to axial movements, rocking could be speculated to be present. In pilot studies using implants with blocked axial motion, the rocking movement was found to be negligible. The ingrowth was similar to stable control implants.

Table 1. Mechanical test of springs (n 14). Mean *SEM*

	Initially	Postimplantation
Stiffness (N/mm)	13.3 *0.77*	15.4 *4.2*
Preload (N)	2.5 *0.08*	2.4 *0.1*
Maximum (N)	4.5 *1.2*	5.2 *1.6*
Displacement (µm)	161 *22*	153 *37*

Stable device

Micromovements could not occur in the stable device. The piston was fixed to the anchorage screw that was inserted into the bone identically with the dynamic device. The polyethylene plug was placed at the level of the articular cartilage surface. Thus, also the stable implant would be loaded during load bearing (Figure 1), but would not be made to move relative to bone.

Implants

The cylindric plugs were 6.0 mm in diameter and 10 mm in length. Ti implants consisted of a solid Ti-6Al-4V alloy core with a coating of Ti-6Al-4V deposited by the plasma spraying technique and a pore size of 200–1,000 µ at the substrate and surface of the coating, respectively. The HA-coated implants consisted of analogous titanium porous-coated implants on which a 50-µm layer of synthetic hydroxyapatite (Ca/P ratio 1.67) was deposited by the plasma-spraying technique. The titanium core for HA coating was appropriately undersized to provide identical implant diameters after coating. X-ray diffraction analysis showed pure hydroxyapatite with no trace of tricalcium phosphate. The polyethylene (UHMWPE) plugs (Chirulen®, Ruhrchemie, Oberhausen, Germany) were 25 µm less than the inner diameter of the centralizer.

Surgical procedures

The operations were performed under general anesthesia. The implantation procedure has been described in detail previously (Søballe et al. 1992). Briefly, the weight-bearing portions of the medial femoral condyles were exposed. The implantation site was selected as the central portion of the femoral condyles, which contacts the meniscus and tibia during the stance and walking phases (Adrian et al. 1966). The stable implants were inserted using an identical

procedure, resulting in static implant loading during gait. The implants were all surrounded by a gap of 0.75 mm permitting free implant movements initially. The dogs were allowed free activity and unrestricted weight-bearing following surgery.

All the dogs regained normal gait within 2–3 days and remained active throughout the study. The dogs were killed after 4 weeks. Ten and 3 days before death, the dogs were tetracycline double-labeled by i.v. administration of chlortetracycline (Dumocyclin®, Dumex, Copenhagen) 15 mg per kg for bone histomorphometry (Frost 1983). Immediately after death, the knees were opened under sterile conditions, the implants exposed, and cultures taken from the implantation site and the synovial fluid. All the polyethylene plugs were in situ. An increased accumulation of synovial fluid was seen in all the knees, but clinical signs of infection were not observed. Bacterial cultures from the implantation site and the synovial fluid obtained after killing the animals were all negative except for sporadic growth of *Pseudomonas* sp. However, a clinical and histologic examination revealed no evidence of acute infection, and these cultures were regarded as being contaminated. Histologic studies of stained synovia showed mild synovial reactions, which were evidenced by the presence of plasma cells and lymphocytes, but no macrophage infiltration was seen.

Preparation

The distal femora were prepared, and standardized sections orthogonal to the long axis of the implant were cut. One 3-mm section was used for mechanical testing, another for histomorphometric and morphologic evaluation on ground, stained specimens, and one for UV fluorescence microscopy.

Mechanical testing

Push-out tests were performed with a universal Instron test machine (Søballe et al. 1989), and load-deformation curves were recorded. Ultimate shear strength, apparent shear stiffness, and energy absorption were estimated from the load-displacement curves (Søballe et al. 1989, 1990, 1991).

Evaluation of fibrous membrane

The membranes around the unstable implants were removed in toto from the surrounding bone under a dissecting stereomicroscope, and standardized biopsies were taken and prepared for histologic examination by light microscopy, transmission electron microscopy, and for determination of hydroxyproline concentration (Figure 2). Two specimens for microscopic analysis and one specimen for hydroxyproline determination from HA-coated implants were lost during preparation.

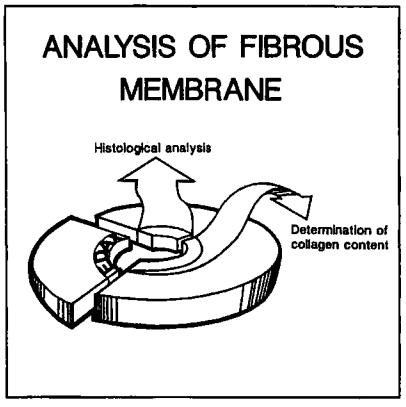

Figure 2. Standardized biopsies of the membrane for histologic analysis, collagen determination, and elemental analysis.

One part of the membrane was prepared for histologic studies, and was stained with toluidine blue at pH 5 for qualitative and quantitative analyses (Figure 2). Fibrocartilaginous tissue in the membrane was quantified using a point-counting technique. Approximately 400 test points were evaluated for each membrane, and an estimate of the percentage of the membrane containing fibrocartilage (chondrocytes) was obtained, with fibrous tissue lacking chondrocytes accounting for the remaining tissue in the membrane.

Standardized specimens (Figure 2) from the membrane were fixed and embedded in epoxy resin and cut to 1-μm-thick slices. A Philips 430 high-resolution electron microscope (HREM) equipped with a STEM-unit and an EDAX 9900 (x-ray energy dispersive analyzer) was used for microanalysis. Using the STEM-unit combined with EDAX, a point element analysis can be obtained from small areas, i.e., the placement of different atoms with an atomic number above 10 can be mapped in the specimen. Such elemental analysis (x-ray mapping) was performed on membranes with specific attention to Ca, P, Ti, Al, and V. Further, the weight percentages of Ca and P were determined. From these values, the Ca/P ratio could be calculated by dividing the weight percentage by the respective molar weight (Ca = 40 g/mol, P = 31 g/mol) at an accuracy of approximately ± 5 percent. Finally, the Ca and P weight percentages were also determined in artificial hydroxyapatite taken from an implant. Four slices were prepared from each specimen; half of them

were stained with uranyl acetate and lead citrate, and the rest were left unstained.

The hydroxyproline concentration was determined on the isolated membranes by a colorimetric method, and the collagen concentration was calculated (Woessner 1976).

Microstructural analysis of the membrane

The fiber orientation in the membranes was studied in 50-μm-thick ground specimens under a transmitted polarizing microscope equipped with a lambda filter.

Histomorphometry

The membrane thickness was measured in 100-μm-thick tissue sections by UV fluorescence microscopy at 100× magnification as the distance between the implant surface and the tetracycline-labeled bone at 10 randomly selected locations around the implant (Kimmel and Webster 1983).

Bone and fibrous-tissue ingrowth. A quantitative histologic evaluation of fibrous-tissue distribution and bone-to-implant apposition was performed on ground, stained specimens at 100× magnification. Specimens were stained with 0.4 percent basic fuchsin and counterstained with 2 percent light green (Gotfredsen et al. 1989). The procedure was performed blindly and in random order using the linear intercept technique. Measurements were made on successive adjacent fields (approximately 300 intercepts) along the entire implant circumference, and an estimate of the percentage of the implant surface in contact with either bone or fibrous tissue was obtained, with bone marrow and empty spaces accounting for the remaining coverage of the implant.

Gap healing. Bone volume was quantified in two well-defined areas from the surface of stable implants (Figure 3) for evaluation of the amount of bone filling the initial gap. The bone volume was estimated blindly by means of a point-counting technique using the central part of the integrating plate with 25 points at 160× magnification. Measurements were made on successive adjacent fields (approximately 800 points) along the entire implant circumference.

Synovium

Specimens of synovium from the knee joint were taken and stained with Giemsa, H&E, and Van Gieson for histologic evaluation of inflammatory changes.

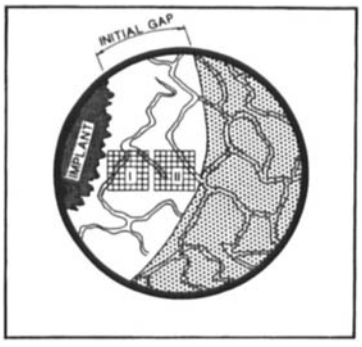

Figure 3. The gap-healing capacity around the stable implants was quantitatively assessed in two well-defined zones from the implant surface. Zone I: 1–6 intersections (i.e., 37–225 μm) from the implant surface. Zone II: 6–11 intersections (i.e., 225–412 μm) from the implant surface. Measurements were made on successive adjacent fields along the entire implant circumference.

Statistics

From all the parameters, the mean values and standard error of the mean (SEM) were calculated. A comparison of the means was performed by two-tailed paired and unpaired *t*-tests. A *P*-value < 0.05 was considered significant. Analyses of variance for repeated measurements were performed on push-out data to determine differences in presence/absence of HA coating and stability.

Results

Mechanical analysis

Push-out test. All the unstable specimens with Ti and HA coating failed between the implant and surrounding fibrous tissue. Most specimens with bony ingrowth (stable implants) failed at the bone-implant interface, but a few stable Ti and HA implants had small amounts of bone on the surface after the push-out test. No failures were observed at the hydroxyapatite-titanium alloy substrate interface.

The ultimate shear strength of unstable Ti and HA implants was reduced compared with the corresponding stable implants ($P < 0.01$). However, shear strength values of unstable HA implants was sevenfold higher than those of unstable Ti implants ($P < 0.01$), and also higher than those of stable Ti implants ($P < 0.01$). The greatest shear strength was obtained by stable HA implants, which exhibited a tenfold stronger anchorage compared with those of stable Ti implants.

Table 2. Mechanical push-out values for titanium- and hydroxyapatite-coated implants under stable and unstable conditions after 4 weeks of implantation (n 7). Mean *SEM*

	Titanium implants				Hydroxyapatite implants			
	Stable		Unstable		Stable		Unstable	
Ultimate shear strength (MPa)	0.73	*0.15*	0.26	*0.07*[a]	7.2	*0.5*[b]	1.85	*0.4*[acd]
Apparent shear stiffness (MPa/mm)	4.1	*1.1*	1.5	*0.4*[a]	71	*6.9*[b]	14.7	*5.2*[acd]
Energy to failure (J/M)	3.8	*0.8*	1.0	*0.3*[a]	33	*6.8*[b]	8.5	*2.1*[acd]

Recording of stiffness and energy absorption failed for one stable titanium implant.
[a]The unstable implant is different from the corresponding stable implant ($P < 0.01$).
[b]The stable hydroxyapatite-coated implant is different from the stable titanium implant ($P < 1 \times 10^{-8}$).
[c]The unstable hydroxyapatite-coated implant is different from the unstable titanium-coated implant ($P < 0.01$).
[d]The unstable hydroxyapatite-coated implant is different from the stable titanium-coated implant ($P < 0.05$).

Shear stiffness and energy absorption showed the same tendency as ultimate shear strength (Table 2). The implants surrounded by a fibrous membrane moved about 80 μm before the contact position was obtained (2 N). The ANOVA showed that the strongest effect of HA coating was obtained during stable mechanical conditions ($F = 97.2$, $P < 0.001$). All the implants loosened between the implant and the membrane during manual removal of the implant from 100-μm specimens.

Histologic studies

The effect of micromovements is illustrated in Figure 4 A where a fibrous membrane has developed around the unstable implant in contrast to the stable implant shown in Figure 4 B, where newly formed bone tissue has filled the initial gap and grown into the surface of the implant.

Unstable implants. All the unstable implants were surrounded by a fibrous membrane. The membranes surrounding the unstable Ti implants consisted predominantly of fibrous connective tissue (Figure 5) without fibrocartilage. Membranes surrounding the HA implants consisted predominantly of small and larger islands of fibrocartilage (Figure 6) with clusters of chondrocytes in lacunae. One membrane consisted solely of fibrous connective tissue. An amorphous purple-stained cartilaginous ground substance was present between the cells. The membranes around Ti implants contained 5 (0–20) percent fibrocartilage, whereas 53 (31–88) percent of the membrane around HA-coated implants consisted of fibrocartilaginous tissue.

At the periphery of the fibrous membrane, a plate of condensed woven bone was concentrically oriented around the implant, which also could be identified on microradiographs. Lymphocytes or macrophages were found especially at the interface between the titanium and membrane.

Stable implants. Bone tissue was in intimate contact with the stable HA implants without interposed fibrous tissue (Figure 7 A). In contrast, stable Ti implants displayed several areas without direct bone-implant apposition and many areas with interposition of fibrous tissue (Figure 7 B). The connective tissue was often arranged parallel to the implant surface. The initial gaps surrounding stable implants were filled by woven bone with high resorptive and formative activity compared with the surrounding bone. No inflammatory reaction was seen around stable implants.

Elemental analysis of fibrous membrane

Around all the instable HA implants, the microanalysis revealed particles with crystalline structure (Figure 8) containing calcium and phosphate (Figure 9) ions. No Ti, V, or Al was found in these membranes. In contrast, all the membranes surrounding unstable Ti implants contained particles with Ti, V, and Al ions. Particles containing calcium phosphate ions were detected in one specimen surrounding a Ti implant. Diffuse calcium phosphate was found in most of the membranes irrespective of type of coating. Phosphate or calcium was never found alone, i.e., when calcium was detected, phosphate was also detected. In one membrane from an HA-coated implant, high concentrations of Al were found, but the Ti concentration was low. The mean Ca/P ratio in the membranes around HA implants was 1.86 (1.69–2.07). The Ca/P ratio from hydroxyapatite coating was 1.65–1.71.

Figure 4 A. Cross section of an unstable HA implant. Note the fibrous membrane around the implant and absence of bone tissue in the initial gap around the implant. Around the periphery of the fibrous membrane, newly formed trabeculae have formed a plate of condensed woven bone concentrically around the implant. This plate of condensed woven bone has a high remodeling activity, as evidenced by many resorptive foci and osteoid formation. Light microscopy, light green, basic fuchsin, ground section, ×6.

Figure 4 B. Cross section of a stable HA implant. Note the newly formed bone has filled the initial gap around the implant. Light microscopy, light green, basic fuchsin, ground section, ×6.

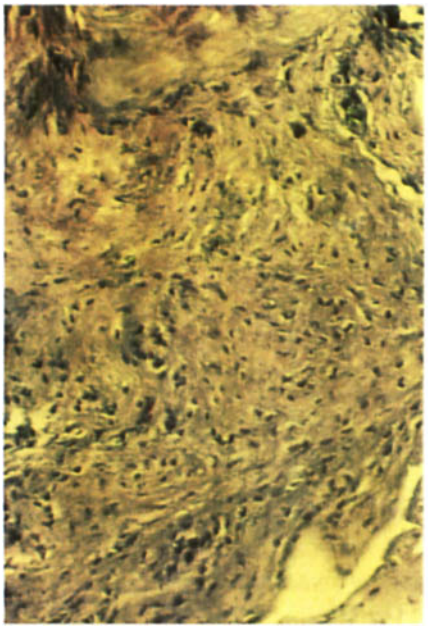

Figure 5. Isolated membrane surrounding an unstable Ti implant showing fibrous connective tissue without fibrocartilage. Light microscopy, toluidine blue at pH 5, ×250.

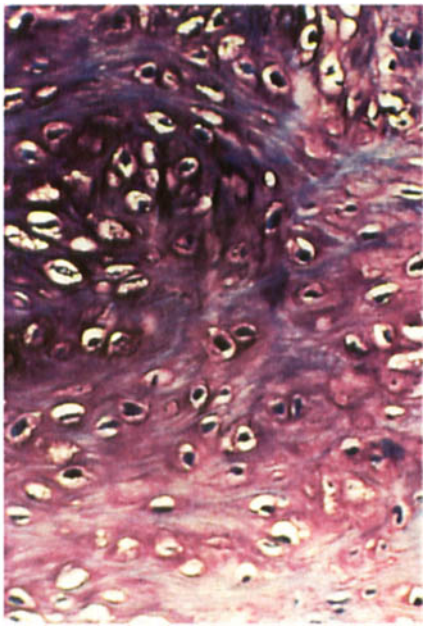

Figure 6. Membrane surrounding an unstable HA-coated implant characterized by islands of fibrocartilage with groups of chondrocytes in lacunae and amorphous purple-stained cartilaginous ground substance. Light microscopy, toluidine blue at pH 5, ×250.

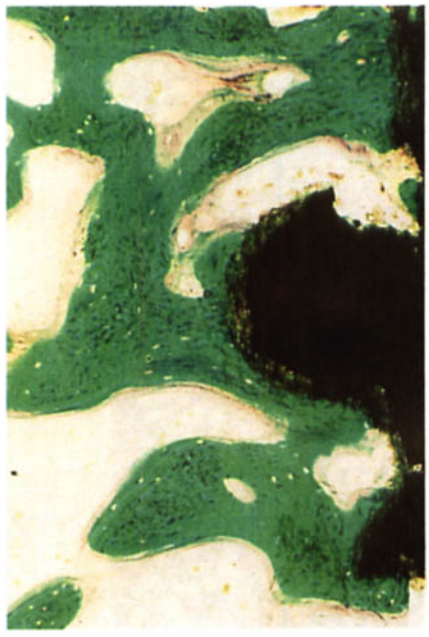

Figure 7 A. Cross section from a stable HA-coated implant showing intimate contact between bone and the hydroxyapatite coating without interposed fibrous tissue layer (light microscopy, light green and basic fuchsin, ×100).

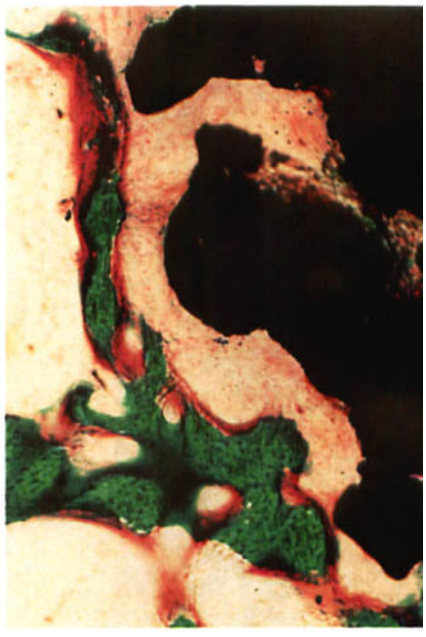

Figure 7 B. Cross section from a stable titanium implant. Note that most of the initial gap is filled with woven bone. Interposed fibrous tissue is attached to the implant surface separating the implant and surrounding bone. Light microscopy, light green and basic fuchsin, ×100.

Figure 8. Diffraction pattern from a particle in the membrane around an HA-coated unstable implant. The electron wave is diffracted in the three-dimensional lattice of atoms, and the regular pattern indicates the crystal nature of the particle. Camera length: 950 mm.

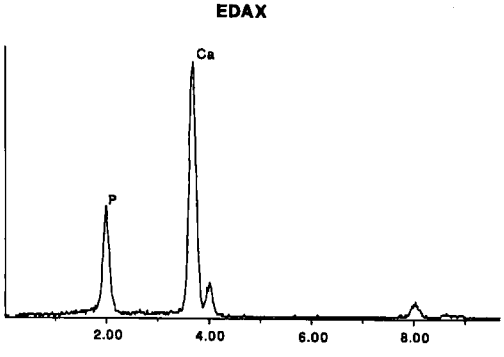

Figure 9. EDAX X-ray energy-dispersive analysis of the area seen in Figure 8 showing peaks representing calcium and phosphate ions. These findings indicate that the particle seen in Figure 8 consists of calcium and phosphate. The Ca/P ratio in this particle was calculated to be 1.8, which approximately corresponds to that measured in artificial HA.

Hydroxyproline determination

The mean collagen concentration in the membrane was 38 percent around titanium implants and 46 percent around hydroxyapatite-coated implants ($P < 0.01$).

Microstructure of fibrous membrane

Fiber orientation. Around unstable HA-coated implants, areas with heavy bundles of collagenous fibers were arranged perpendicular to the implant surface (Figure 10 A and B). The collagen fibers

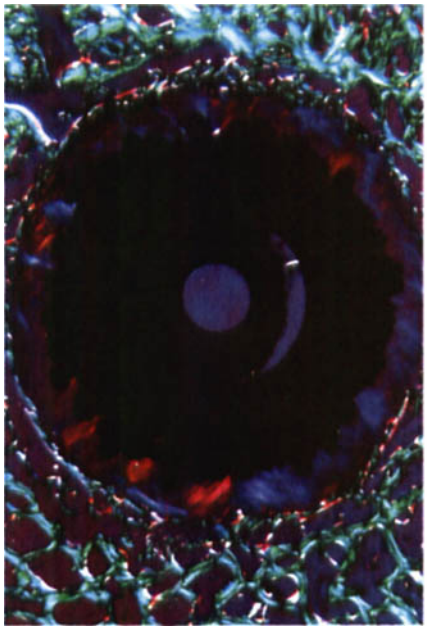

Figure 10 A. Polarized light micrograph of an unstable hydroxyapatite-coated implant showing the alignment of heavy bundles of collagenous fibers radiating perpendicular to the implant surface. The collagen fibers extend to the implant from the well-defined plate of condensed woven bone surrounding the membrane. Polarizing microscopy, light green and basic fuchsin, ×8.

Figure 10 B. Close-up view of Figure 10A (light microscopy without polarization). The collagenous fibers extend fan-shaped from the implant surface toward the surrounding bone. Note the precipitates of granulated material stained positive for light green located between the fibers, suggesting that the membrane contains calcium phosphate. The fibers are oriented toward a lacuna (pore) in the implant surface to terminate on an area of mineralized bone growing directly on the HA coating. Light microscopy, light green and basic fuchsin, ×100.

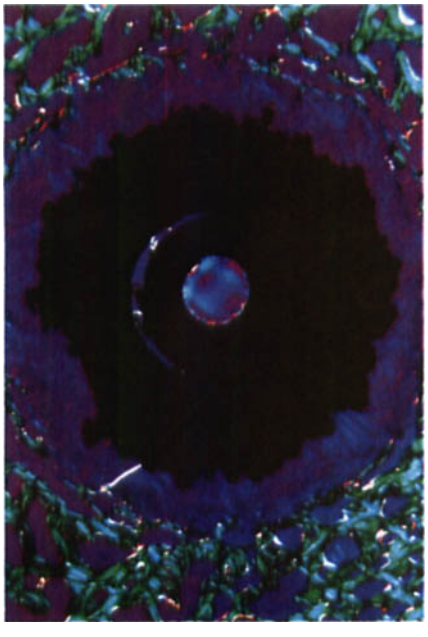

Figure 10 C. Polarized micrograph of an unstable titanium implant showing random orientation of thin collagenous fibers. Structures positively stained for light green is not demonstrated. Polarizing microscopy, light green and basic fuchsin, ×8.

extended to the implant from a condensed bone plate of woven bone that surrounded the membrane. In these ligament-like bundles, granulated material stained positive for light green, indicating the occurrence of precipitates of calcium phosphate. The fibers were often oriented toward lacunae in the implant surface to terminate in an area of mineralized bone growing directly on the HA-coated surface (Figure 10 B). In other cases, the fibers ended directly on the HA coating. Around unstable titanium implants, a more random orientation of thinner collagenous fibers was found (Figure 10 C), but a few samples showed the same tendency to arrange the fibers radially from the implant surface. Structures positively stained for light green were only seen sporadically. Mineralized bone was not found at the unstable Ti implant surfaces.

Histomorphometry

Thickness of fibrous membrane around unstable implants. The membrane was thicker around Ti-coated implants compared with HA-coated implants,

Table 3. Bone ingrowth (percentage) of the implant surface in direct contact with bone (n 7). Mean *SEM*

Titanium implants		Hydroxyapatite implants	
Stable	Unstable	Stable	Unstable
13 *3*	0[a]	65 *2*[b]	7 *2*[a]

[a] The unstable implant is different from the corresponding stable implant ($P < 1 \times 10^{-7}$).
[b] The stable hydroxyapatite-coated implant is different from the stable titanium implant ($P < 1 \times 10^{-7}$).
No difference between the unstable HA and the stable Ti implant.

Table 4. Fibrous tissue ingrowth (percentage) of the implant surface in direct contact with fibrous tissue (n 7). Mean *SEM*

Titanium implants		Hydroxyapatite implants	
Stable	Unstable	Stable	Unstable
57 *9*	89 *3*[a]	0[b]	82 *3.5*[a]

[a] The unstable implant is different from the corresponding stable implant ($P < 0.001$).
[b] The stable hydroxyapatite-coated implant is different from the stable titanium implant ($P < 0.0001$).
No difference between the unstable HA and the stable Ti implant.

Table 5. Gap healing (bone volume; percentage; n 7; see Figure 3). Mean *SEM*

Titanium implants		Hydroxyapatite implants	
Stable	Unstable	Stable	Unstable
Zone 1			
26 *2.5*	0.6 *0.4*[a]	41 *1.6*[b]	2.3 *1.3*[a]
Zone 2			
25 *1.8*	0.9 *0.3*[a]	32 *2.5*[b]	7.6 *2.3*[acd]

[a] The unstable implant is different from the corresponding stable implant ($P_{Zone\ 1} < 0.00001$, $P_{Zone\ 2} < 0.0001$).
[b] The stable hydroxyapatite-coated implant is different from the stable titanium implant ($P_{Zone\ 1} < 0.001$, $P_{Zone\ 2} < 0.05$).
[c] The unstable hydroxyapatite-coated implant is different from the unstable titanium implant ($P < 0.01$).
[d] The unstable hydroxyapatite implant is different from the stable titanium implant ($P < 0.00001$).
No difference between the unstable HA and stable Ti implant in *Zone 1*.

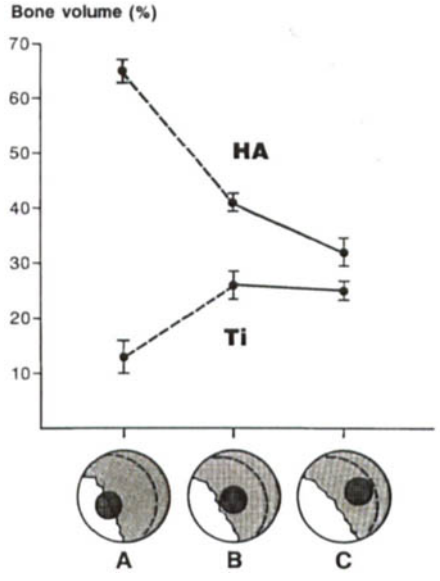

Figure 11. Quantitative evaluation of the gap-healing capacity around stable implants in two well-defined areas from the implant surface. For location of zones I and II, see Figure 3.
A. Bone coverage on implant surface (see Table 3).
B. New bone formation in the initial gap in zone I (see Table 5).
C. New bone formation in the initial gap in zone II (see Table 5).
Note the positive gradient of newly formed bone toward the hydroxyapatite-coated surface, which was not found toward the titanium coating.
The dotted lines indicate different units:
A. Bone coverage of the implant surface (percentage).
B and C. Bone volume (gap healing; percentage).

averaging 524 (17) and 360 (17) µm, respectively ($P < 0.0001$).

Bone and fibrous tissue ingrowth. Bone ingrowth into stable HA implants increased fivefold compared with Ti-coated implants (Table 3). The mean fibrous tissue coverage was 57 percent of Ti implants, whereas no fibrous tissue was found on HA-coated surface (Table 4).

No bone was found in direct contact with unstable titanium-coated implants, but an average of 7 percent of the HA-coated surfaces were covered by bone (Table 3). An equal amount of fibrous tissue covered the unstable Ti- and HA-coated implants (Table 4).

Gap healing. HA coating increased the gap-healing capacity under both stable and unstable conditions compared with Ti coating. Negligible amounts of bone had filled the initial gap around unstable Ti implants. In contrast, a greater ($P < 0.01$) amount of bone was found around unstable HA implants (Table 5).

Around stable implants the HA coating further stimulated newly formed bone in the initial gap at some distance from the surface of the coating compared with Ti coating (Figure 11). A positive gradient of newly formed bone was found toward the HA coating, which was not found toward the Ti coating.

Cancellous bone structure around the membrane

In the surrounding bone around unstable implants, a high remodeling activity was seen that increased toward the bone-membrane interface, as evidenced by many resorptive foci and osteoid formation. The high remodeling activity at the periphery of the membrane was further demonstrated by accumulation of tetracycline-labeled bone at the border of the drill hole. Many osteoblasts were seen at the border between membrane and surrounding bone where both bone resorption and bone formation occurred, the latter by woven bone. A zone of condensed woven bone was seen at the entire circumference around the membrane (Figure 4 A).

Discussion

Micromotion and fibrous membrane

This study indicates that implant movements approximating 150 µm during each gait cycle may inhibit bone ingrowth and result in development of a fibrous membrane. Our findings are in agreement with a previous study on 500-µm movements using an identical experimental model producing micromovements during each gait cycle (Søballe et al. 1990, 1992). An interesting finding was the stronger anchorage of unstable than stable implants when HA coating was used despite the fact that the HA implants were surrounded by a thick fibrous membrane. Studies on bioactive ceramics have shown that collagen is structurally integrated within the crystallized apatite (Hench 1988). If the collagen fibers are similarly embedded and bonded within the surface of the hydroxyapatite used in the present study, the stronger fibrous anchorage of unstable HA-coated implants when compared with those of stable and unstable Ti implants could be explained by a stronger bonding capacity of collagen to HA.

Therefore, the explanation could be a stronger bonding between collagen and the HA surface compared with that of the Ti surface despite the fibrous layer around stable Ti implants being much thinner than those around unstable HA implants.

Orientation of collagen fibers

The radiating orientation of collagen fibers containing calcium phosphate precipitations around unstable HA-coated implants might also contribute to increased implant fixation compared with the more random collagen orientation around Ti implants. Differences between fiber orientation around Ti- and HA-coated implants could not be evaluated quantitatively, as the analysis of fiber orientation was purely qualitative. However, the radiating fiber orientation might be similar to those described in other studies where oblique fiber orientation to the implant surface was found in membranes from a loaded Co-Cr-Mo intramedullary model (Pilliar 1981) and a porous-coated Ti segmental prosthesis (Heck et al. 1986).

The fiber orientation probably reflects the load transfer by the fibrous layer. Because the movements of Ti- and HA-coated implants were equal, at least initially, a direct or indirect effect on fiber orientation seems to be mediated by the HA coating. The ligament-like structures around HA-coated implants could be compared with the periodontal ligament (Lindhe 1989), which serves as the only fixture of the tooth root to the surrounding bone. The finding that the fiber bundles often terminate in an area of mineralized bone growing on the HA coating might be comparable with the attachment of the periodontal ligament to the tooth cementum—a part of the periodontal ligament (Sharpey's fibers) is embedded in the cementum and is mineralized.

The strong attachment of collagen fibers to bone formed on the HA coating or to the HA coating itself indicates a higher degree of biocompatibility of HA for collagen than that of Ti alloy. Although the collagen fibers were well attached to the HA implant, there was a stronger mechanical connection between the membrane and surrounding osseous tissue, because all the manually removed implants loosened between the implant and the membrane.

Direct bone formation on HA surface

The ability of new bone to form directly on the surface of the HA coating (shown in Figure 10 B) seems to be advantageous, as collagen fibers may have a stronger attachment to mineralized bone tissue than to Ti metal without bone growth on the surface. The presence of bone growing directly on the HA surface supports the hypothesis by Geesink et al. (1987) and Jarcho (1981) that gaps around HA-coated implants are filled by two ossification fronts, one from the implant surface toward the surrounding bone and the other from surrounding bone toward the implant.

The presence of pores on the HA surface also seems to be advantageous, for new bone formation always was present in these pores of unstable implants, which indicates that HA should be coated on to a porous metal coating to facilitate bone formation even during unstable mechanical conditions.

Collagen concentration and fibrocartilage

The greater collagen concentration and presence of fibrocartilage around the HA implants are consistent with our previous finding (Søballe et al. 1990, 1992). They also indicate that HA coating has a stimulatory effect on collagen synthesis in the membrane that might contribute to increased fibrous anchorage of HA-coated implants, as fibrocartilage with a high collagen content may be expected to have relatively stronger mechanical properties than connective tissue (Bloom and Fawcett 1975).

The different types of fibrous tissue around the two implant types may represent different phases of endochondral ossification, where an inflammatory phase is followed by differentiation of cartilage and increased collagen production. Thus, membranes around HA implants might represent a later phase in endochondral ossification, and new bone formation bridging the initial gap between the bone and the HA implant might have developed if the observation period had been longer. This is in agreement with the interfragmentary strain theory (Perren 1979): viz., that the presence of fibrocartilage may reduce the movements between bone and implant to a level where bone formation is possible.

Brown et al. (1989) have shown that bone ingrowth occurs via direct bone formation in press-fit inserted implants. However, when bone ingrowth has been prevented by implant movements, fibrocartilaginous tissue has been observed (Sumner and Galante 1990). In a recent clinical study, Ryd and Linder (1989) reported on three stable cemented Marmor knee arthroplasties revised 5–7 years after insertion for reasons other than mechanical loosening. They found fibrocartilage at the central part of the supporting tissue, and suggested that presence of fibrocartilage around the prosthesis provided adequate support for a clinical successful course. Their findings are in agreement with Pauwels' (1980) theory that cells differentiate into chondroblasts in regions of high hydrostatic pressure.

Calcium phosphate crystals in membrane

The presence of light-green-stained precipitations in membranes around unstable HA-coated implants led us to further investigations of the membrane using electron microscopy equipped with EDAX for chemical elemental analysis. This examination revealed new results concerning biological reactions on HA coating, because calcium phosphate crystals were demonstrated in all the membranes around the HA-coated implants, whereas only one membrane around the Ti implants contained calcium phosphate crystals. These findings support the histologic findings of calcium/phosphate precipitations in the membranes around HA-coated implants, and confirm that these precipitations are calcium phosphate crystals. The elemental analysis revealed Ca/P ratios (1.86) close to that of artificial HA (1.67), as measured by the same procedure. However, other values were also found indicating that different calcium salts were present in the membrane. Precipitation of calcium phosphate crystals in the membrane around HA implants may originate from dissolved calcium phosphate from the HA coating, which has been suggested to occur in vivo (van Blitterswijk et al. 1986, Beight et al. 1989). The finding could also indicate that the calcium phosphate originated from resorbed, surrounding bone, as the elemental analysis cannot differentiate between calcium phosphate crystals originating from surrounding bone and from dissolved HA. The presence of calcium phosphate precipitations in the membrane surrounding HA implants is an interesting finding and might be an early manifestation of new bone formation. However, studies with longer observation periods are in progress to clarify this suggestion.

Metal ion release inhibited by HA

The presence of particles containing Ti, Al, and V ions in the membranes around Ti-alloy implants in the present study was not surprising, because in vitro and in vivo (Agins et al. 1988) studies have documented the release of metal ions from Ti-6Al-4V alloy implants. HA coating seems to prevent, or at least reduce, the release of metal ions from the metal substrate (Ducheyne and Healy 1988). In an in vitro study, Ducheyne and Healy (1988) showed that the release of titanium, aluminum, and vanadium ions was reduced by a thin layer of plasma-sprayed hydroxyapatite coating. The dispersion of metal fragments into the surrounding fibrous tissue during specimen preparation could have contributed to the metal content observed around Ti implants in the present study, but because the cores of both implant types consisted of Ti alloy, metal ions would also have been detected around HA-coated implants if the source had been contamination during preparation. Thus, HA coating seems to prevent release of metal ions within the 4 weeks' implantation period.

Gap healing capacity

Under stable conditions, HA coating increased the gap healing capacity of bone compared with Ti coating even at a relatively great distance from the hydroxyapatite surface. This finding indicates that the osteoconductive effect of HA is not limited to the bone-forming capacity on the surface of the implant. Our finding may support Beight et al. (1989), who suggested that a calcium phosphate coating acts by providing a local source of Ca and PO_4 ions essential for mineralization of the surrounding tissue.

Effect of porous surface

The location of newly formed bone on the unstable HA-coated implants was primarily in the pores of the surface, and may be explained by a more steady mechanical milieu, as these areas on the rough surface of the implant are not fully exposed to the unstable mechanical milieu. However, no bone was found on unstable Ti implants, which had an even rougher surface with deeper pores than the HA surface. This suggests that a steady mechanical milieu is not the only determining factor for new bone formation, and that the type of surface coating plays an important role for bone formation.

Effect of stress on stable implants

The anchorage and amount of bone ingrowth as seen in this study on stable HA-coated implants were threefold greater than those reported in a previous study using the same type of implantation technique (Søballe et al. 1990, 1992). Differences in stress on the implant in the two studies probably explain the different amounts of bone ingrowth on HA implants, for the stable implants in the previous study (Søballe et al. 1990, 1992) were unloaded during the 4-week observation period. Thus, they were stress shielded in contrast to those of the present study, where the stable implants were loaded during the whole observation period. These findings are in agreement with Turner et al. (1986), who suggested that underloading (stress shielding) results in inferior bone ingrowth and cortical resorption around the implant. Jasty and Harris (1988) also showed the importance of loads on rigidly fixed acetabular components, as unloaded components showed inferior bone ingrowth when compared with loaded components.

Acknowledgements

The authors wish to acknowledge Allan Henschel, Ph.D., Laboratory of Applied Physics, Building 307, Technical University of Denmark, DK-2800 Lyngby, Denmark, for performing the microanalysis of the membranes; Professor Flemming Melsen, M.D., Ph.D., University Institute of Pathology, Århus Amtssygehus, Denmark, for advise in histomorphometric analysis; Peter H Jørgensen, M.D., Department of Connective Tissue Biology, Institute of Anatomy, University of Århus, Denmark, for the determination of the collagen concentrations; Lis Mosekilde M.D., Institute of Anatomy, University of Århus, Denmark, for the loan of the polarizing microscope; Ms. Jane Pauli and Anette Milton, Royal Dental College, Århus, Denmark, for technical assistance with the grinding procedure. Biomet Inc., U.S.A., kindly provided the implants.

Financial support was obtained from the Danish Rheumatism Association, Danish Medical Research Council, Institute of Experimental Clinical Research, University of Århus, Århus University Research Foundation, Danish Foundation for the Advancement of Medical Science, Direktør Madsen og hustrus Olga Madsens Fond, Ferd. og Ellen Hindsgauls Fond, and Kong Kristian Den Tiendes Fond.

References

Adrian M J, Roy W E, Karpovich P V. Normal gait of the dog: an electrogoniometric study. *Am J Vet Res* 1966; 27 (116): 90–5.

Agins H J, Alcock N W, Bansal M, Salvati E A, Wilson P D Jr, Pellicci P M, Bullough P G. Metallic wear in failed titanium alloy total hip replacements. A histological and quantitative analysis. *J Bone Joint Surg* (Am) 1988; 70 (3): 347–56.

Beight J, Radin S, Cuckler J, Ducheyne P. Effect of solubility of calcium phosphate coatings on mechanical fixation of porous ingrown implants. *Trans of the 35th Ann Meet Orthop Res Soc* 1989; 14: 334.

van Blitterswijk C A, Grote J J, Kuijpers W, Daems W T, de Groot K. Macropore tissue ingrowth: a quantitative and qualitative study on hydroxyapatite ceramic. *Biomaterials* 1986; 7 (2): 137–43.

Bloom W, Fawcett D W. *A textbook of histology*. W B Saunders Co, Philadelphia, 10th ed 1975.

Branson P J, Steege J W, Wixson R L, Lewis J, Stulberg S D. Rigidity of initial fixation with uncemented tibial knee implants. *J Arthroplasty* 1989; 4 (1): 21–6.

Brown C C, McLaughlin R E, Balian G. Intramedullary bone repair and ingrowth into porous-coated implants in the adult chicken: a histologic study and biochemical analysis of collagens. *J Orthop Res* 1989; 7 (3): 316–25.

Burke D W, O Connor D O, Zalenski E B, Jasty M, Harris W H. Micromotion of cemented and uncemented femoral components. *J Bone Joint Surg* (Br) 1991; 73 (1): 33–7.

Ducheyne P, Healy K E. The effect of plasma sprayed calcium phosphate ceramic coatings on the metal ion release from porous titanium and cobalt-chromium alloys. *J Biomed Mater Res* 1988; 22 (12): 1137–63.

Geesink R G, de Groot K, Klein C P. Chemical implant fixation using hydroxyl-apatite coatings. The development of a human total hip prosthesis for chemical fixation to bone using hydroxyl-apatite coatings on titanium substrates. *Clin Orthop* 1987; 225: 147–70.

Gotfredsen K, Budtz Jörgensen E, Jensen L N. A method for preparing and staining histological sections containing titanium implants for light microscopy. *Stain Technol* 1989; 64 (3): 121–7.

Heck D A, Nakajima I, Kelly P J, Chao E Y. The effect of load alteration on the biological and biomechanical performance of a titanium fiber-metal segmental prosthesis. *J Bone Joint Surg* (Am) 1986; 68 (1): 118–26.

Hench L L. Bioactive ceramics. In: *Bioceramics: Material characteristics versus in vivo behaviour* (eds: Ducheyne P and Lemons J E) *Ann N Y Acad Sci 1988;* 523: 54–71.

Jarcho M. Calcium phosphate ceramics as hard tissue prosthetics. *Clin Orthop* 1981; 157: 259–78.

Jasty M, Harris W H. Observations on factors controlling bony ingrowth into weight-bearing, porous, canine total hip replacements. In: *Non-cemented total hip replacement* (Ed. Fitzgerald Jr R) Raven Press Ltd, New York 1988: 175–89.

Kimmel D B, Webster S S J. Measurements of area, perimeter, and distance: details of data collection in bone histomorphometry. In: *Bone histomorphometry: Techniques and interpretion.* (Ed. Recker R R) CRC Press Inc, Boca Raton, Florida 1983: 89–108.

Lindhe J. *Textbook of clinical periodontology.* 2nd ed. Munksgaard, Copenhagen 1989.

Pauwels F. A New theory concerning the influence of mechanical stimuli on the differentiation of supporting tissue. In: *Biomechanics of the locomotor apparatus* (Ed. Pauwels F) Springer Verlag, New York 1980: 375.

Perren S M. Physical and biological aspects of fracture healing with special reference to internal fixation. *Clin Orthop* 1979; 138: 175–96.

Pilliar R M, Cameron H U, Welsh R P, Binnington A G. Radiographic and morphologic studies of load-bearing porous surfaced structured implants. *Clin Orthop* 1981; 156: 249–57.

Ryd L, Linder L. On the correlation between micromotion and histology of the bone-cement interface. Report of three cases of knee arthroplasty followed by roentgen stereophotogrammetric analysis. *J Arthroplasty* 1989; 4 (4): 303–9.

Shimagaki H, Bechtold J E, Sherman R, Gustilo R B. Initial stability of tibial components in cementless total knee arthroplasty. *Trans 34th Ann Meet Orthop Res Soc* 1988; 13: 477.

Strickland A B, Chan K H, Andriacchi T P, Miller J. The initial fixation of porous coated tibial components evaluated by the study of rigid body motion under static load. *Trans 34th Ann Meet Orthop Res Soc* 1988; 13: 476.

Sumner D R, Galante J O. Bone growth. In: *Surgery of the musculoskeletal system.* (Ed. Evarts C Mc C) 2nd Ed, Churchill Livingstone, New York 1990: 151–76.

Søballe K, Hansen E S, Brockstedt Rasmussen H, Hjortdal V E, Juhl G I, Pedersen C M, Hvid I, Bünger C. Enhancement of osteopenic and normal bone ingrowth into porous-coated implants by hydroxyapatite coating. *Trans 35th Ann Meet Orthop Res Soc* 1989a; 14: 385.

Søballe K, Hansen E S, Brockstedt Rasmussen H, Pedersen C M, Bünger C. Early fixation of allogenic bone graft in titanium and hydroxyapatite-coated implants. *Trans 35th Ann Meet Orthop Res Soc* 1989b; 14: 554.

Søballe K, Hansen E S, Brockstedt Rasmussen H, Jørgensen P, Bünger C. Hydroxyapatite coating provides a stronger fibrous anchorage of implants with controlled micromotion. *Trans 36th Ann Meet Orthop Res Soc* 1990a; 15: 206.

Søballe K, Hansen E S, Brockstedt Rasmussen H, Pedersen C M, Bünger C. Hydroxyapatite coating enhances fixation of porous-coated implants. A comparison in dogs between press fit and noninterference fit. *Acta Orthop Scand* 1990b; 61 (4): 299–306.

Søballe K, Hansen E S, Brockstedt Rasmussen H, Hjortdal V E, Juhl G I, Pedersen C M, Hvid I, Bunger C. Fixation of titanium and hydroxyapatite-coated implants in osteopenia. *J Arthoplasty* 1991c; 6 (4): 307–16.

Søballe K, Hansen E S, Brockstedt Rasmussen H, Hjortdal V E, Juhl G I, Pedersen C M, Hvid I, Bünger C. Gap healing enhanced by hydroxyapatite coating in dogs. *Clin Orthop* 1991d; 272: 300–7.

Søballe K, Hansen E S, Brockstedt Rasmussen H, Jørgensen P, Bünger C. Tissue ingrowth into titanium and hydroxyapatite-coated implants during stable and unstable mechanical conditions. *J Orthop Res* 1992a; 10: 285–9.

Søballe K, Hansen E S, Brockstedt Rasmussen H, Pedersen C M, Bünger C. Bone graft incorporation around titanium-alloy and hydroxyapatite-coated implants. *Clin Orthop* 1992b; 274: 282–93.

Turner T M, Sumner D R, Urban R M, Rivero D P, Galante J O. A comparative study of porous coatings in a weight-bearing total hip arthroplasty model. *J Bone Joint Surg* (Am) 1986; 68 (9): 1396–409.

Vanderby R, Manley P A, Kohles S S, Belloli D M, McBeath A A. A micromotion comparison of cemented and porous ingrowth total hip replacements in a canine model. *Trans 35th Ann Meet Orthop Res Soc* 1989; 14: 577.

Volz R G, Nisbet J K, Lee R W, McMurtry M G. The mechanical stability of various noncemented tibial components. *Clin Orthop* 1988; 226: 38–42.

Woessner J F. Determination of hydroxyproline in connective tissues. In: *The methodology of connective tissue research.* (Ed. Hall D A), Joynsson Bruvvers, Oxford 1976: 227–33.